

# NCAM Is Essential for Axonal Growth and Fasciculation in the Hippocampus

Harold Cremer,\* Genèviève Chazal,\* Christo Goridis,\* and Alfonso Represa†

\*Laboratoire de Génétique et Physiologie du Développement, IBDM, CNRS/INSERM/Université de la Méditerranée, Campus de Luminy, Case 907, F-13288 Marseille Cedex 9, France; and †INSERM U 29, Hôpital Port-Royal, 123 Boulevard Port Royal, F-75674 Paris Cedex 14, France

The neural cell adhesion molecule (NCAM), probably the best characterized and most abundant cell adhesion molecule on neurons, is thought to be a major regulator of axonal growth and pathfinding. Here we present a detailed analysis of these processes in mice deficient for all NCAM isoforms, generated by gene targeting. The hippocampal mossy fiber tract shows prominent expression of polysialylated NCAM and the generation of new axonal projections throughout life. Focusing on this important intrahippocampal connection, we demonstrate that in the absence of NCAM, fasciculation and pathfinding of these axons are strongly affected. In addition we show alterations in the distribution of mossy fiber terminals. The phenotype is more severe in adult than in young animals, suggesting an essential role for NCAM in the maintenance of plasticity in the mature nervous system.

## INTRODUCTION

Interactions among cells are essential for the development of functional connections in the vertebrate nervous system. Cell–cell and cell–substrate adhesion (reviewed by Jessell, 1988; Rutishauser and Jessell, 1988; Hynes and Lander, 1992) as well as chemoattraction and repulsion (reviewed by Tessier-Lavigne, 1994) have been shown to provide the basis for these processes, and a variety of molecules have been identified which mediate these interactions (reviewed by Goodman and Shatz, 1993). The neural cell adhesion molecule (NCAM) was the first molecule mediating cell adhesion that was identified on the basis of functional criteria (Thiery *et al.*, 1977; reviewed by Edelman, 1988). A variety of isoforms of this immunoglobulin superfamily member are generated by alternative splicing, differing in the size of their cytoplasmic domains, their mode of membrane attach-

ment, or the structure of the extracellular domains (reviewed by Goridis and Brunet, 1992). In addition to this variability at the protein level, NCAM has been described as the major, if not the exclusive, carrier of  $\alpha$ -2,8-linked polysialic acid (PSA) (reviewed by Rougon, 1993), an unusual carbohydrate structure thought to promote axonal growth and adult neuronal plasticity (reviewed by Seki and Arai, 1993b; Rougon, 1993).

NCAM appears during early embryonic development on derivatives of all three germ layers (reviewed by Goridis and Brunet, 1992). After birth, it becomes essentially restricted to neural tissues. On the basis of its highly regulated expression pattern, roles in processes such as neurulation (Bally-Cuif *et al.*, 1993), axonal growth (Tosney *et al.*, 1986), retinal histogenesis and generation of its projections (Thiery *et al.*, 1977; Silver and Rutishauser, 1984), and development of the olfactory system (Key and Akesson, 1990; Chung *et al.*, 1991) have been postulated. The best characterized function of NCAM, mainly relying on *in vitro* assays and on the injection of antibodies or of the PSA-removing enzyme Endo N, is its ability to promote and regulate neurite outgrowth (Doherty *et al.*, 1990a,b) and fasciculation (Rutishauser, 1988; Tang *et al.*, 1994; Yin *et al.*, 1995).

To approach NCAM function *in vivo* we used targeted inactivation of the NCAM gene to generate mice lacking all protein isoforms (Cremer *et al.*, 1994). The phenotype of these mice, but also of mice lacking only the NCAM-180 isoform (Tomasiewicz *et al.*, 1993), appeared to be surprisingly mild. These animals were found to have a size-reduced olfactory bulb, due to a defect in migration of olfactory neuron precursors (Ono *et al.*, 1994; Hu *et al.*, 1996), and deficits in spatial learning and exploratory behavior (Cremer *et al.*, 1994). More recently, another

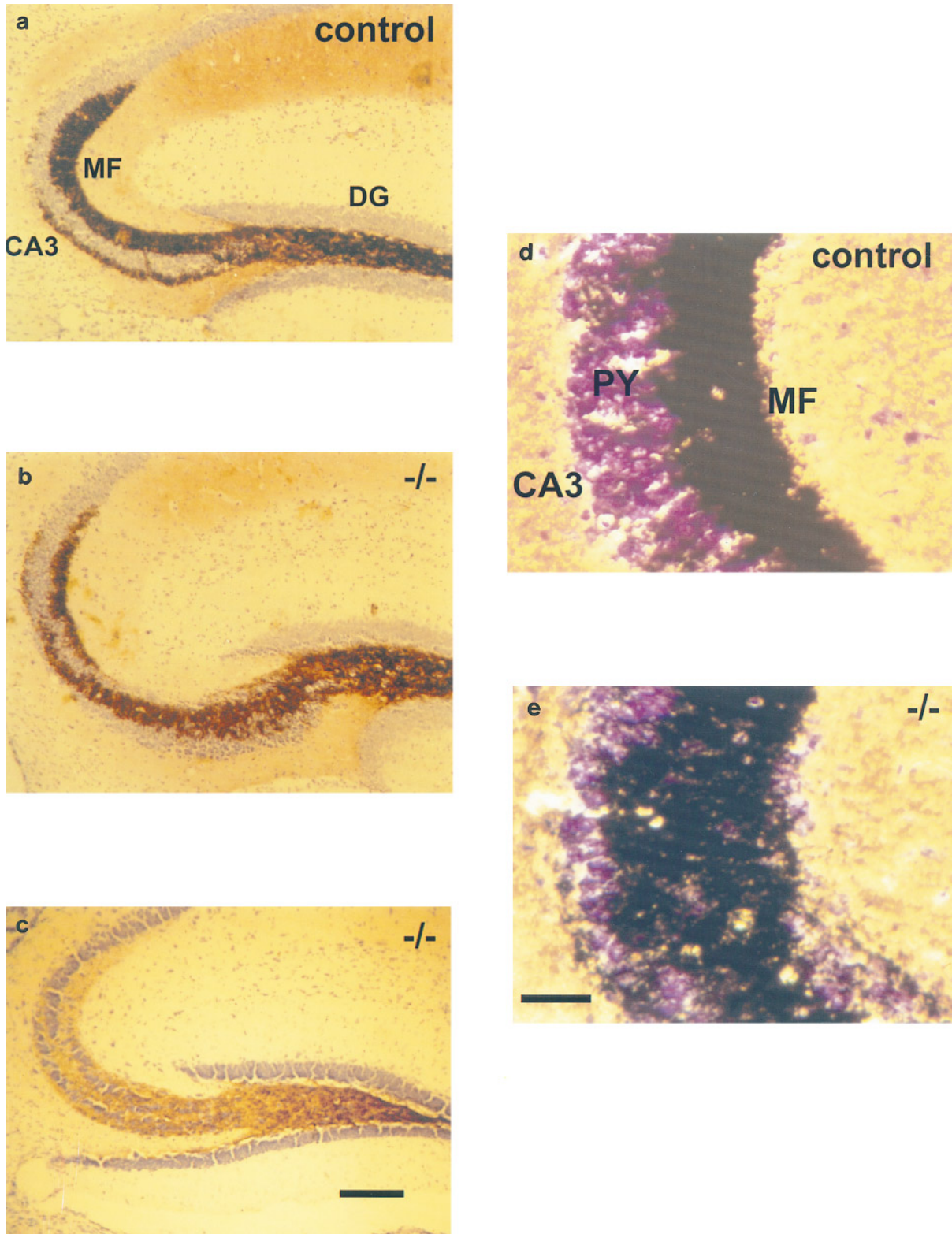


**FIG. 1.** Analysis of the mossy fiber tracts of adult wild-type and  $NCAM^{-/-}$  mice. Sagittal sections of the hippocampus were stained by Timm's method to reveal mossy fibers and counterstained with cresyl violet, which stains most prominently the granule and pyramidal cell layers. Control mice (a) showed, in all cases, the typical strong and ordered labeling of the mossy fibers which appear almost black. (b,c) Mossy fiber staining of

study revealed deficient long-term potentiation in the hippocampus (Muller *et al.*, 1996). NCAM<sup>-/-</sup> mice are almost totally devoid of PSA, demonstrating that NCAM is by far the major carrier of this carbohydrate (Cremer *et al.*, 1994).

The olfactory system is one of the few sites in the mammalian brain where neurogenesis and prominent expression of PSA persist in the adult (Seki and Arai, 1993b; Rousselot *et al.*, 1995). Here we present a detailed analysis in NCAM-deficient mice of another brain structure with ongoing neurogenesis (Kaplan and Hinds, 1977; Kuhn *et al.*, 1996) and high PSA-NCAM expression (Seki and Arai, 1993a,b; Cremer *et al.*, 1994): the dentate gyrus of the hippocampus and its axonal projection, the mossy fibers (mfs). The mfs are the axons of the neurons which form the granule cell layer of the dentate gyrus. Each of them grows a single axon, which forms *en passant* synapses with the proximal dendrites of the pyramidal cells in the CA3 region of the hippocampus (Amaral and Witter, 1995; Cowan *et al.*, 1980). We demonstrate that pathfinding and laminar growth of the mfs are strongly affected in the absence of NCAM and present evidence that the basis for these alterations may be deficient fasciculation. These results provide genetic proof for a vertebrate cell adhesion molecule playing a key role in axonal growth and pathfinding.

## RESULTS

### *Altered Distribution and Loss of Mossy Fibers in Adult NCAM-Deficient Mice*

We used Timm's staining which specifically reveals mfs and most prominently their synaptic expansions (Haug, 1973) to study mf deposition in NCAM<sup>-/-</sup> and control mice. Wild-type and heterozygous adult mice show a strong and homogeneous staining of the mfs as they form *en passant* synapses with the apical and basal dendrites of the CA3 pyramidal cells (Fig. 1a). In the CA3 region, the mfs are mainly confined to the suprapyramidal tract, i.e., the apical dendritic region of the pyramidal cells, forming a layered structure. Only in the

region close to the hilus do the mfs course across the pyramidal cell layer as shown by Timm's staining. Most of the mfs in the suprapyramidal tract appear to reach the CA3-CA2 border as indicated by the undiminished staining intensity there (Figs. 1a and 1d). In contrast, adult NCAM<sup>-/-</sup> animals show a reduced staining intensity and striking alterations in the distribution of the fibers. In the most severe cases, the remaining fibers seem to fade out before reaching the end of the CA3 region and are strongly disorganized, invading the pyramidal cell layer and destroying its laminar appearance. In these cases, cresyl violet staining reveals a dispersed and broken-up pyramidal cell layer (Fig. 1c). In less affected mutants, there is still prominent mf staining along the entire CA3 region, but in all animals analyzed, staining intensity is reduced, the fibers appear disorganized, and the characteristic layering is disturbed (Figs. 1b and 1e).

To quantify the loss of mfs in NCAM-deficient mice, we analyzed the optical density of Timm-stained sections generated from adult 3- to 4-month-old control and mutant mice. We devised a rigorous protocol to obtain topologically equivalent and comparably stained sections (see Experimental Methods). Equivalent areas which included hilus, stratum oriens, stratum lucidum, and CA3 pyramidal cell layer, thus all mf-containing structures, were measured in all animals. This analysis revealed a statistically significant overall 20% loss of mfs in adult mutants compared to controls (Fig. 2).

Even in quantitatively less affected mutants, Timm's staining is more diffuse and distributed over a wider area, suggesting reduced bundling of mfs in the absence of NCAM. To reveal mfs by an independent technique, which visualizes the axons themselves rather than their synaptic expansions, we used immunohistochemistry with antibodies against the axonal markers neurofilament heavy chain (Figs. 3a and 3b) and tau (Figs. 3c and 3d). Although the labeling is less specific than Timm's staining, it reveals in both cases thick bundles of fibers in the wild-type animals, whereas in the mutants, the immunoreactivity is not that well organized and distributed over a wider area.

---

two different mutants to present examples of a weak (b) and a strong (c) phenotype. The penetrance of the phenotype shows some degree of variability, especially in staining intensity (compare b and c). However, an altered pattern of mossy fiber distribution is found in all mutants analyzed. The axons invade the pyramidal cell layer, not respecting their normal laminar organization. A typical observation is that the staining fades out along the innervated area. (d,e) High magnifications of mutant and control CA3 regions show the growth of fibers between the pyramidal cells and their spreading over a wider area, suggesting reduced fasciculation, which is never seen in the wild type in this region. The mutant shown represents a less affected case with near normal mossy fiber density, yet presenting a clearly abnormal axonal trajectory. CA3, hippocampal CA3 region; DG, dentate gyrus; MF, mossy fibers; PY, pyramidal cell layer. (a-c) Bar, 200  $\mu$ m; (d,e) bar, 50  $\mu$ m.

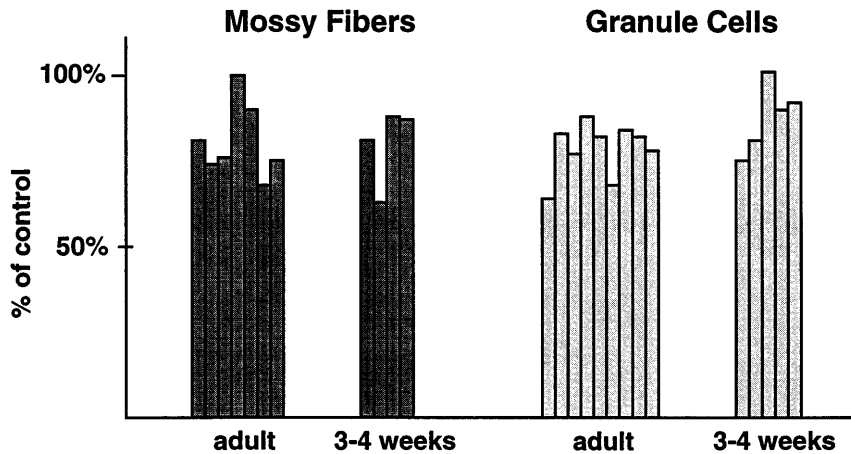


**FIG. 2.** Quantitative analysis of mossy fiber and granule cell density. The mf number was estimated by measuring the optical density of Timm-stained serial sagittal sections of the hippocampus. Granule cell number was determined by measuring the surface area of the granule cell layer on cresyl violet-stained serial sagittal sections. The bars represent the values obtained for individual young or adult mutant animals, expressed in percentage of the optical density or surface area on level-matched sections from control mice, processed in the same experiment. Mean values were for mf density in adult mutants:  $80.3 \pm 4.2\%$ ,  $n = 7$ ,  $P < 0.004$ ; in 3- to 4-week-old animals:  $77.3 \pm 8.3\%$ ,  $n = 4$ ,  $P \leq 0.03$ . For the granule cell number in adult mutants:  $78.4 \pm 2.6\%$ ,  $n = 9$ ,  $P < 0.0001$ ; in 3- to 4-week-old animals:  $88.2 \pm 4.2\%$ ,  $n = 5$ ,  $P < 0.05$ .

### **Golgi Staining Reveals a Loss of Mossy Fiber Terminals on CA3 Neurons**

We used the Golgi technique to visualize individual pyramidal cells in the CA3 area. The mfs terminate on the pyramidal cell dendrites on particular large spines, the so-called “thorny excrescences . . . ,” . . . representing the postsynaptic parts of the mf terminals (Cowan *et al.*, 1980; Amaral and Witter, 1995). A lack of mf terminals in the mutant hippocampus, as indicated by reduced Timm’s staining, should lead to a visible loss of these structures. Figure 4 shows representative pyramidal neurons from the CA3 region. Whereas in wild-type animals the dendrites appear heavily loaded with excrescences, in the mutant situation, there are consistently fewer of these characteristic structures. In addition to these quantitative changes, the area on the apical dendrites on which excrescences are found usually appears larger and the spines more widely distributed than in controls. Altogether the observation of individual neurons confirms the defects in mf innervation, which may be expected on the basis of the altered Timm’s staining.

### **The mf Defect Is Less Severe in Young Animals**

The granule cells of the dentate gyrus have been shown to be generated and to extend axonal projections in the form of mfs throughout adult life (Kaplan and Hinds, 1977; Stanfield and Trice, 1988; Kuhn *et al.*, 1996). We wanted to establish whether the alterations seen in the adult were already present at earlier stages or were

exclusively due to deficits of the late-generated axons. Timm’s staining of 3- to 4-week-old mutants, when the main features of hippocampal structural organization have just been laid down (Cowan *et al.*, 1980; Amaral and Dent, 1981), already shows alterations in the mf pattern. Reduced staining intensity and some misrouting of fibers in the CA3 region are visible, but the staining appears more homogeneous along the mf pathway than in adults (Figs. 5a and 5b).

Quantitative analysis revealed that there was about the same 20% overall loss of mfs in young and adult (see above) mutants (Fig. 2). To investigate changes of mf distribution over the termination field more precisely, we quantified Timm’s staining of the passing fibers in three equally sized areas of the CA3 region. Optical density was expressed in relation to area 1, located in the proximal region of the mf pathway close to the hilus (Fig. 6a). There was an approximately 50% decrease in staining intensity along the mf innervation field in both 3- to 4-week-old mutants and control animals (Fig. 6b). This value is comparable to the approximately 40% decrease found for the adult controls (Fig. 6c), indicating that in all three cases, at least half of the axons reach the proximal region of their termination field. However, in adult NCAM<sup>-/-</sup> mice, only about 25% of the mfs reach the CA3–CA2 border (Fig. 6c), verifying quantitatively the fading-out effect described above. Hence, although mfs are already reduced in number and somewhat disorganized in young animals, signs of premature termination are not yet apparent.

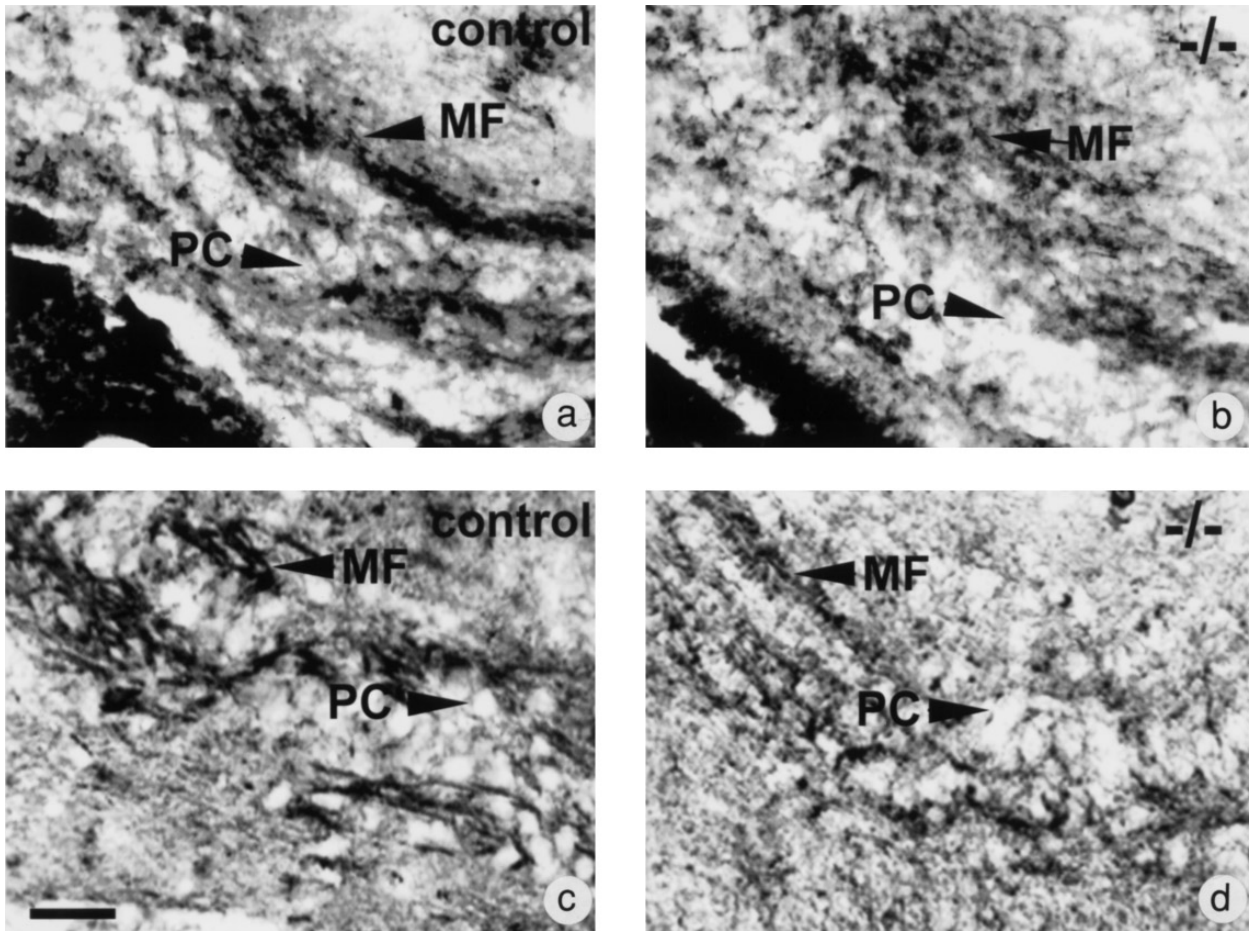


**FIG. 3.** Neurofilament and tau immunohistochemistry of NCAM<sup>-/-</sup> (b,d) and control (a,c) hippocampi. Sagittal sections of the hippocampus stained for neurofilament heavy chain (a,b) and tau (c,d). A loss of fibers in the region of the mossy fiber tract is visible in the mutant (b,d) compared to the control (a,c). In addition, the axon bundles appear to be less fasciculated in the NCAM-deficient situation showing a more diffuse staining for the neurite markers. MF, mossy fiber; PC, pyramidal cell. Bar, 50  $\mu$ m.

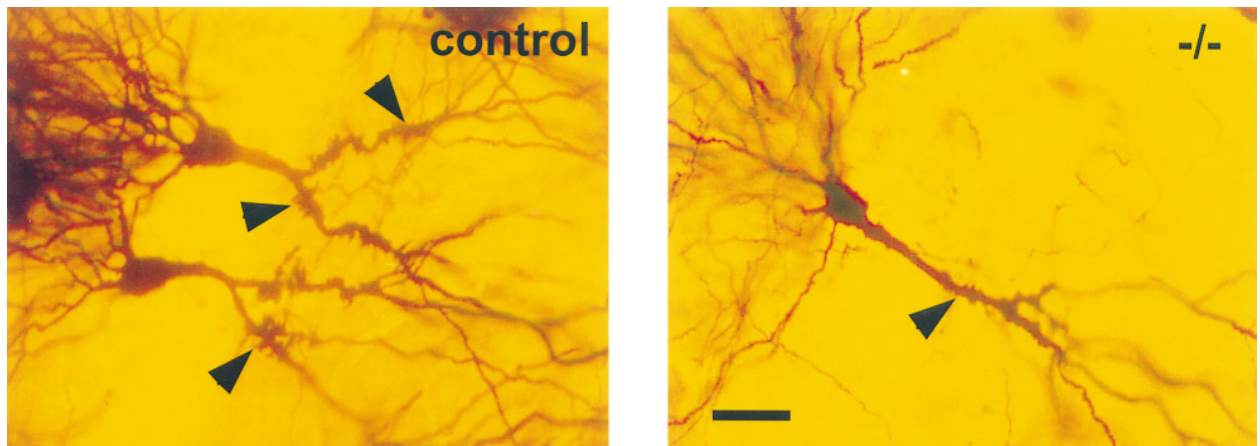


**FIG. 4.** Golgi staining of pyramidal neurons. Individual pyramidal neurons from an equivalent region from the middle of the CA3 area are shown. Thorny excrescences on the apical dendrites of pyramidal neurones (arrowheads) are visible in both cases, but are more abundant in the control (left). Notice the broader distribution of excrescences in the mutant (right) compared to control. Bar, 25  $\mu$ m.

### The Loss of mfs Is Not Due to a Deficit in Granule Cell Generation

A deficit in the number of mfs could be the consequence or the cause of a loss of the granule cells from which they arise. We thus estimated granule cell number by measuring the area of the granule cell layer in serial sections. This can be taken as a measurement of granule cell number since the surface area occupied by individual granule cells is the same under all conditions (not shown). In adult NCAM-deficient mice, there was a 20% size reduction of the granule cell layer, hence a 20% reduction in granule cell number, a decrease similar to that measured for mf density (Fig. 2). However, in

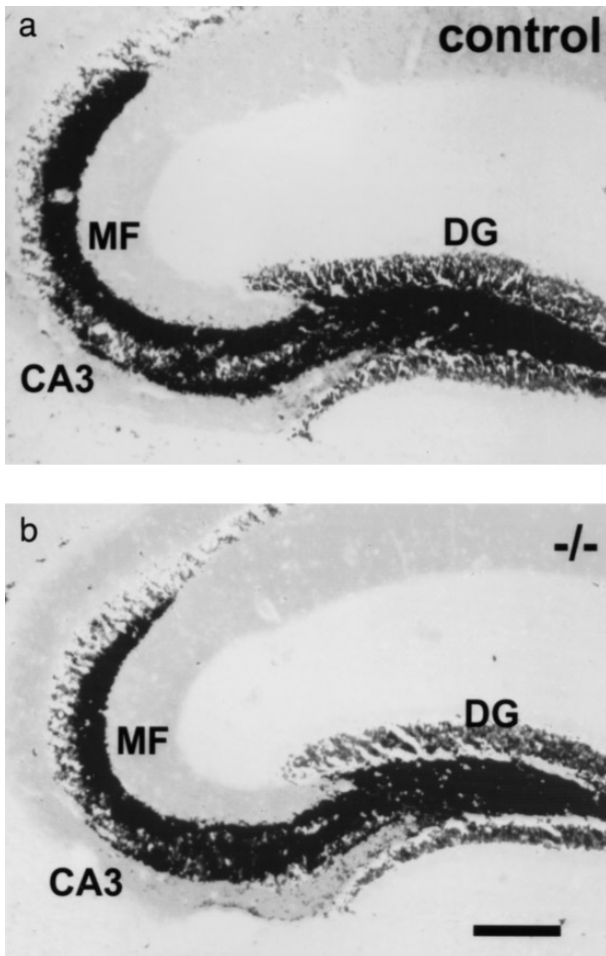


**FIG. 5.** Analysis of the mossy fiber pathway of 4-week-old NCAM<sup>-/-</sup> (b) and control (a) mice. Although the Timm-staining pattern appears more homogeneous and laminated in younger mutants, the basic characteristics of the phenotype are already visible: a quantitative reduction and ingrowth of mossy fibers between the pyramidal cells in more proximal regions. CA3, CA3 region; DG, dentate gyrus; MF, mossy fibers. Bar, 200  $\mu$ m.

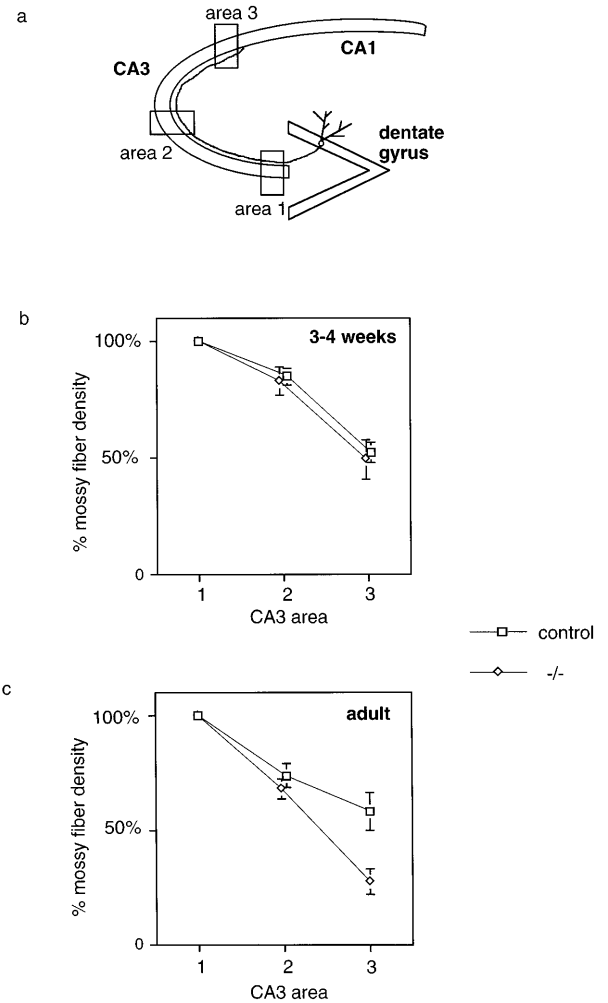


**FIG. 6.** Quantitative analysis of changes in mossy fiber distribution along their innervation field. (a) Schematic representation of the analyzed areas in sagittal hippocampal sections stained by Timm's method. The measured areas include the CA3 pyramidal cell layer, the stratum lucidum, and the stratum oriens, thus all passing mossy fibers. Morphological landmarks were used to choose strictly equivalent areas from all sections. Values are shown as percentage of staining in area 1, which was set at 100%. (b) Analysis of 3- to 4-week-old control and NCAM<sup>-/-</sup> animals. No difference in the distribution of mossy fibers between control and mutant animals was visible along the innervation field (controls,  $52.0 \pm 4.3\%$ ,  $n = 6$ ; -/-,  $49.0 \pm 8.0\%$ ,  $n = 5$ ). (c) Analysis of adult animals. Controls show essentially the same innervation pattern as the younger animals with over 50% of the mossy fibers attaining the most distal CA3 area ( $58.0 \pm 8.1\%$ ,  $n = 5$ ). In the mutants, there is a significantly greater decline of staining density over the innervation field with only about 25% of the fibers reaching area 3 ( $27.4 \pm 5.4\%$ ,  $n = 7$ ).

young mutants we found an approximately 10% reduction in granule cell number, suggesting that the loss of these neurons might be secondary to the deficit in axonal growth and synaptogenesis.

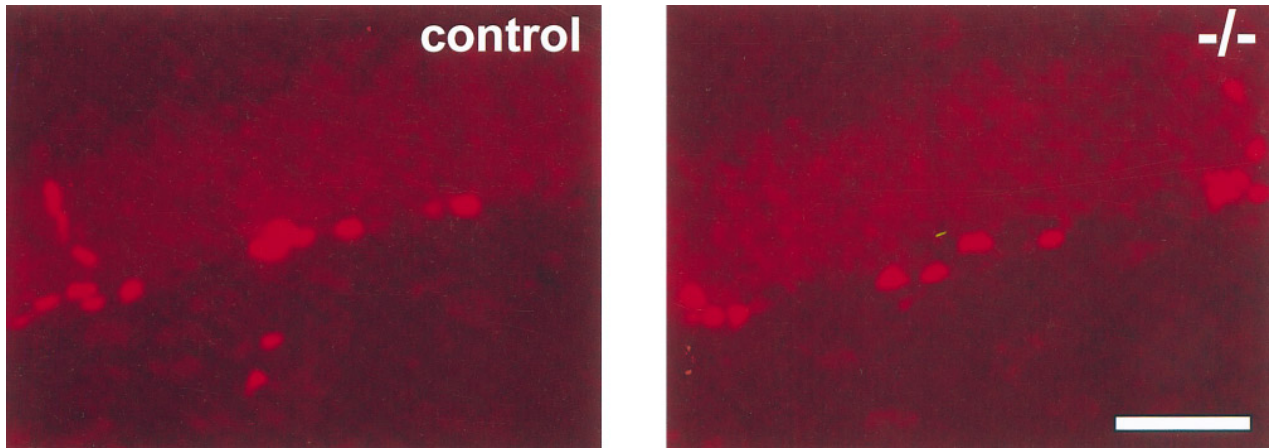


**FIG. 7.** BrdU immunohistochemistry of mutant (right) and control (left) dentate gyrus. Quantity and deposition of BrdU-labeled cells was indistinguishable between both groups. Most of the labeled cells appear in the subgranular zone and the innermost layer of the dentate gyrus, but in both cases some immunoreactive cells appear in the granule cell layer itself. Quantitatively, no difference between the groups was found. Bar, 50  $\mu$ m.

To approach this question, we injected 2- to 3-month-old NCAM<sup>-/-</sup> and control mice with 5-bromo-2'-deoxyuridine (BrdU) to label newly generated granule cells. After four BrdU injections over a 48-h period, the animals were perfused, and hippocampal sections were stained with anti-BrdU antibodies. Labeled cells in three to four level-matched sections from NCAM-deficient and control mice were counted. This analysis revealed no significant difference in the number of labeled cells per section between both groups (control:  $33.8 \pm 2.5$ ,  $n = 3$ ; mutant:  $36.1 \pm 2.1$ ,  $n = 3$ ;  $P > 0.19$ ). Also, the topographical distribution of the labeled cells at the border of the hilus region appeared indistinguishable (Fig. 7). Labeled cells were found along the entire granule cell layer, in the subgranular zone of the dentate gyrus, and in the deep portion of the granule cell layer itself. In sections from both groups, we found individual labeled cells integrated into the granule cell layer.

#### **Ultrastructural Evidence for Altered Fasciculation of NCAM-Deficient Mossy Fibers**

Electron microscopy was used to investigate the ultrastructure of the hippocampal CA3 region. Figures 8A and 8C represent the typical organization of mf fascicles in this area. Thick bundles of the nonmyelinated mfs are seen in proximity to the pyramidal cell bodies and dendrites. No axon terminals or dendritic spines are present inside the fascicles (Fig. 8A). When cut transversally (Fig. 8A), the axons appear densely packed with the membranes in very close apposition. The relatively homogeneous diameters of the transver-

sally cut fibers suggests a high degree of parallel orientation. This parallel organization is also indicated by the large number of longitudinally sectioned bundles as shown in Fig. 8C, where axons travel over long distances in close contact with each other.

The organization of this region is strikingly different in the NCAM-deficient situation. Figures 8B and 8D are images of comparable areas from mutant mice. Here, the mfs seem to be almost totally unfasciculated and appear intermingled with synaptic terminals and dendritic spines (Fig. 8B). Only in very few cases can bundle-like structures be seen, but they appear less densely packed and show fewer direct membrane contacts. In addition, the variable fiber diameters indicate a lack of parallel orientation (Fig. 8D, center). As one would expect from this observation, strictly longitudinally sectioned fascicles, as in Fig. 8C, are never seen in the mutants. Altogether, the altered ultrastructural organization appears in perfect accordance with the evidence gained from the altered and diffuse staining seen in Timm- and immunohistochemically stained sections (Figs. 1 and 3).

## **DISCUSSION**

Cell adhesion molecules expressed in neural tissues have been implicated in the control of axonal growth, fasciculation, and pathfinding, but genetic evidence that the "classical" vertebrate cell adhesion molecules do actually fulfill these functions *in vivo* has not been reported to date. A role for NCAM in these processes has been suggested by a large body of evidence, based

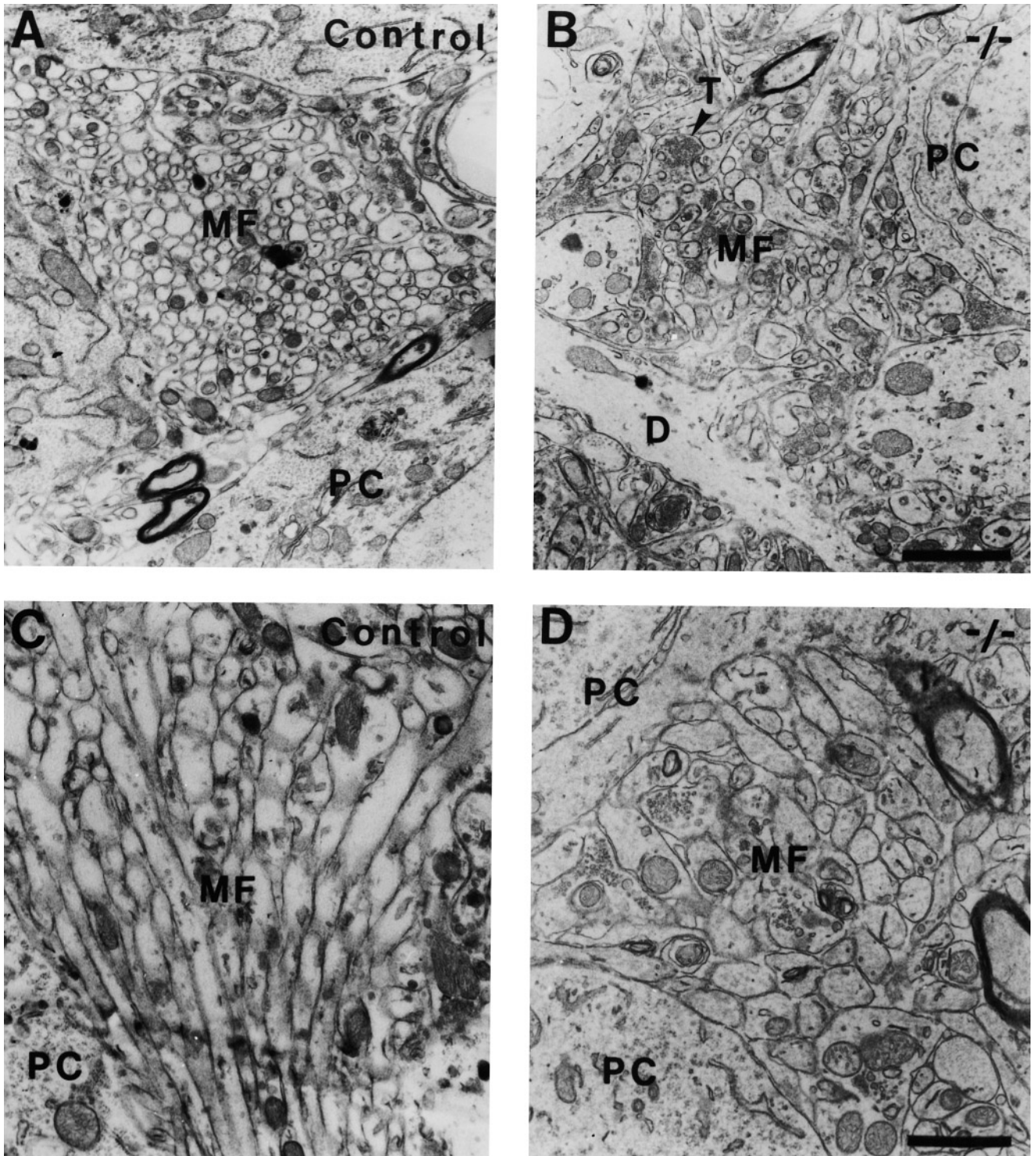


**FIG. 8.** Ultrastructural analysis of mf organization in mutant (B,D) and control (A,C) mice. Control mice show a high degree of fasciculation with fibers densely packed and in a strictly parallel orientation (A,C). No terminals are found inside the mf bundles which appear highly homogeneous when transversally sectioned (A). In the absence of NCAM, the fibers seem to grow individually (B), and only in a few cases, small bundle-like structures can be identified (D). Notice the closer membrane apposition in the controls and lower degree of direct contact in the mutants (compare C and D). Mf terminals (T), which appear grossly normal, and dendritic spines appear between the fibers which were never seen in the controls. In addition, longitudinally cut axon bundles, as in C, are never seen in mutants, probably due to the lack of parallel orientation of fibers. MF, mossy fibers; PC, pyramidal cell; T, mossy fiber terminal. (A,B) Bar, 2  $\mu$ m; (C,D) bar, 1  $\mu$ m.

on experiments with cultured cells and on injection of antibodies and modifying enzymes into living animals. In one experimental paradigm, the capacity of NCAM to promote or to inhibit neurite outgrowth and the modulation of these processes by PSA was shown using primary neurons growing on monolayers which express different isoforms of NCAM after transfection (Doherty *et al.*, 1990a,b). In another one, removal of PSA was shown to reduce neurite outgrowth on NCAM-expressing membrane vesicles (Zhang *et al.*, 1992). Other *in vitro* experiments suggest the involvement of receptor (Williams *et al.*, 1994) or nonreceptor (Beggs *et al.*, 1994) tyrosine kinases in NCAM-mediated signaling, which would account for the cellular responses leading to neurite outgrowth.

*In vivo* evidence for a role of NCAM in axonal growth control has relied on the injection of adhesion-blocking anti-NCAM antibodies or of the neuraminidase Endo N, which specifically removes PSA from NCAM. Examples of antibody effects include the perturbation of optic fiber projections to the tectum (Fraser *et al.*, 1988; Yin *et al.*, 1995) or of chicken hindlimb innervation (Landmesser *et al.*, 1988). The use of Endo N to perturb NCAM function has led to somewhat contradictory results. Whereas the enzymatic removal of PSA increased bundling of motor neuron axons in the periphery (Tang *et al.*, 1994), it has exactly the opposite effect in the CNS: a striking defasciculation as demonstrated for chick retinal ganglion cells (Yin *et al.*, 1995) and spinal cord neurons (Rutishauser *et al.*, 1988). However, these experiments are fraught with many problems, such as limited access of the reagents, steric interference with other membrane proteins or incomplete blocking of protein function (Grenningloh and Goodman, 1992). A potentially even more serious problem is the ability of antibodies to trigger signaling pathways (Schuch *et al.*, 1989). Hence, effects ascribed to antibody inhibition may in fact be due to inappropriate triggering of intracellular signals.

The genetic approach using targeted inactivation of the NCAM gene overcomes these problems. Nevertheless the phenotype of these mice appeared remarkably mild at first sight (Tomasiewicz *et al.*, 1993; Cremer *et al.*, 1994). Size reduction of the olfactory bulb, which could be traced back to a deficit in granule cell migration (Hu *et al.*, 1996), and behavioral defects were the only documented abnormalities. Here we show that mice lacking all NCAM isoforms indeed show an abnormal axonal growth pattern in the hippocampal mf pathway. Our main findings include an overall reduction in mf density, a failure of mfs to reach their final target area at the CA3–CA2 border, and, most strikingly, disorganized growth of the mf bundles which invade and disrupt the

pyramidal layer, probably because of a lack of fasciculation. In adult mutants, the decrease in mossy fiber density was of the same magnitude as the reduction in granule cell number. Granule cell proliferation was, however, not affected by the mutation. Thus we are left with the interpretation that the primary defect is the altered mf growth pattern which secondarily leads to a loss of granule cells. This interpretation is also supported by our observation that the granule cell deficit, but not the overall reduction in mf density, was less pronounced in young mice.

Upon leaving the hilus region, mfs normally travel in three major tracts. Some grow deep to the CA3 pyramidal cells, in the infrapyramidal bundle of stratum oriens, some course within the pyramidal cell layer in the intrapyramidal bundle, but most take a route superficial to the CA3 pyramidal neurons in the suprapyramidal bundle, which forms the major constituent of stratum lucidum. All fibers eventually join the stratum lucidum and reach the CA3–CA2 border (Amaral and Witter, 1995). This ordered organization is severely altered in the NCAM-deficient situation, despite the fact that all axons initially grow in the right direction and appear to make synapses with their correct target neurons, the CA3 pyramidal cells. With Timm's staining, mfs are seen coursing between the pyramidal cell bodies also in the distal CA3 region. The diffuse staining seen with Timm's method or with immunohistochemistry of axonal markers as well as our ultrastructural analysis point to defasciculation of mf bundles as the basic defect, in a way comparable to the Endo N effects mentioned above.

So far genetic evidence for a role of a neural cell adhesion molecule in axonal pathfinding has been provided only in *Drosophila* (reviewed by Grenningloh and Goodman, 1992; Garrity and Zipursky, 1995). The loss-of-function phenotype of fasciclin II (Grenningloh *et al.*, 1991; Lin *et al.*, 1994), an insect relative of NCAM, is reminiscent of the phenotype we describe. In *fasII* mutants, axons still extend in the correct direction, but certain axon bundles fail to form. Defasciculation of these tracts seems to be the primary event leading to disorganization of axon fascicles and neuropil.

Many questions remain unanswered as to how NCAM functions to mediate orderly growth and fasciculation of mfs. One is how it functions in the context of other cell adhesion molecules that may act synergistically or antagonistically. Of particular interest is the description of the limbic system-associated protein (LAMP), also a member of the immunoglobulin superfamily and expressed mostly on neurons of the limbic system (Levitt, 1984). Intraventricular administration of anti-LAMP antibodies results in abnormal growth of mossy fibers

(Pimenta *et al.*, 1995). These changes include defasciculation and invasion of the pyramidal cell layer, a phenotype highly reminiscent of the one we describe. Lack of NCAM might well influence LAMP-mediated functions in the hippocampus, in a way similar to the NCAM interactions with L1 documented in other systems (Kadmon *et al.*, 1990; Landmesser *et al.*, 1988; Tang *et al.*, 1994).

Another question is whether the phenotype we observe may be attributed to the lack of PSA, since the mfs are one of the few structures where PSA-NCAM persists into adulthood (Seki and Arai, 1993a,b). PSA is thought to have an inhibitory effect not only on NCAM-mediated recognition events but also on cell interactions depending on other molecules (Rutishauser *et al.*, 1988; Acheson *et al.*, 1991). A PSA-mediated inhibition of cell-cell adhesion seems at odds with our finding of decreased fasciculation in its absence. However, our results are not without precedent, as defasciculation of axon bundles after enzymatic removal of PSA has been observed, both *in vitro* (Acheson *et al.*, 1991) and *in vivo* (Yin *et al.*, 1995). This has been attributed to a shift from axon-axon to axon-substratum interactions in a situation where axons and their environment carry PSA as in the developing optic tract (Yin *et al.*, 1995). However, the mfs grow in a PSA-negative environment (Seki and Arai, 1993a) and form intimate contact only with each other, not with other cells or an acellular environment. Thus, we favor the idea that NCAM has an essential function in driving the fasciculation of the axons, possibly by influencing the activity of other cell adhesion molecules such as LAMP, be it via interactions in the plane of the membrane or via transmembrane signaling. Similarly, defasciculation seen after PSA removal may be due to a functional perturbation of axonal NCAM rather than to a shift in the balance between axon-axon and axon-substrate adhesion.

The two structures affected in NCAM-deficient mice, the granule cell layer of the olfactory bulb and the mf system of the hippocampus, are characterized by their postnatal development and persisting neurogenesis. The phenotype suggests that NCAM is essential for neural morphogenesis and the orderly growth of axons after birth, whereas its function can be taken over by other cell adhesion molecules in the embryo. This interpretation is supported by our observation that the mutant phenotype was less severe in young than in fully mature mice. Late outgrowing mfs might depend more on guiding cues provided by fasciculation with their forerunners to find their way through the densely packed neural elements of the adult hippocampus than the first generated axons, which navigate through a

more permissive environment. Hence, NCAM may subserve an essential function in regions of adult neuronal plasticity.

Neuronal plasticity is thought to be important in learning and memory, and inhibition of such processes may underlie the reported effects of NCAM deficiency and Endo N treatment (Muller *et al.*, 1996) as well as of anti-NCAM antibodies (Luthi *et al.*, 1994) on hippocampal long-term potentiation. Furthermore, strain-dependent variations in hippocampal mossy fiber distribution have been shown to be correlated with spatial learning abilities and exploratory behavior in mice (Schwegler *et al.*, 1988; van Daal *et al.*, 1991; Jamot *et al.*, 1994). NCAM-deficient mice have been demonstrated to be impaired in both of these cognitive tasks (Cremer *et al.*, 1994), and the changes in mf growth and pathfinding demonstrated here might well represent the physiological basis for this behavioral deficit.

## EXPERIMENTAL METHODS

### Animals

NCAM-deficient mice were described previously (Cremer *et al.*, 1994). All analyses were performed on animals with two genetic backgrounds: either C57BL/6J (four backcrosses) or 129. No differences according to genetic background were found. For quantitative analysis, results obtained with both lines were pooled. In all cases heterozygous and wild-type animals were indistinguishable.

### Timm's Staining

Control and mutant animals were perfused through the heart with the equivalent of one body weight of sodium sulfide solution (Haug, 1973) followed by fixation with the same amount of 4% paraformaldehyde (PFA). Twenty-micrometer-thick sections were cut on a cryostat. Mounted sections were stained in darkness at 24°C using the conditions described by Haug (1973). The staining was terminated after 15 min, when mfs appeared strongly stained but saturation was not yet achieved. A fraction of the sections was counterstained with cresyl violet to observe cellular organization. After postfixation in photofixative (Kodak), the sections were dehydrated, mounted, and coverslipped.

### Quantitative Analysis

For quantification of mossy fiber density, only animals perfused and stained side by side using the same

solutions were compared. Great care was taken to section the brains in a strictly equivalent plane. Every 10th section was stained by the Timm's method and the optical density of at least three level-matched sections per animal was measured. Size and form of the lateral ventricle, striatum, and dentate gyrus were used as morphological landmarks for level matching. Measures were performed using a light microscope linked to an image analysis system (Imasys) where the parameters were set to avoid saturation of the gray scale. The analyzed area included hilus, stratum oriens, stratum lucidum, and CA3 pyramidal cell layer, thus all mf-containing structures. Statistical significance was determined by Student's *t* test.

To determine granule neuron number in the dentate gyrus, the surface area of the granule layer was measured on cresyl violet-stained serial sagittal sections using the same image analysis setup. To prevent the possibility that differences in cell density or size were influencing the measurement, individual cells were counted after Hoechst 33258 labeling of the nuclei and the area occupied by individual cells was estimated. No difference for this parameter was detectable between wild-type and mutant animals.

### Immunohistochemistry

Animals were perfused with 4% PFA and treated as described above. Immunocytochemical staining was performed on floating sections in TBS containing 0.1% Triton X-100 using monoclonal antibodies against neurofilament heavy chain (Sigma N 4142) and tau protein (Sigma T 5530). The staining reaction used biotinylated secondary antibodies and the Vectastain ABC kit (Vector).

### Golgi Staining

For the modified Golgi (Spacek, 1989) technique, the mice were perfused with 4% PFA/2% glutaraldehyde in PBS. Vibratome sections (100  $\mu$ m) were placed for 24 h in 2.4% potassium dichromate containing 0.2% osmium tetroxide before incubation in 0.75% silver nitrate solution for another 24 h. Sections were dehydrated, cleared with xylene, and mounted with Permount.

### BrdU Labeling

The mice were given four injections of BrdU (60 mg/g body weight, ip; Sigma) over 2 days. Perfusion and preparation of sections was performed, as described above, 6 h after the last injection. Sections were denatur-

ated in a buffer containing 2 N HCl, 0.5% Triton X-100 in PBS for 10 min and neutralized by washing in 0.1 M sodium tetraborate. After saturation in DMEM containing 15% FCS, sections were incubated overnight with mouse anti-BrdU antibody (Sigma; 1:100) before detection with Texas red-conjugated secondary antibody. Labeled cells in three to four level-matched sections of each animal were counted.

### Electron Microscopy

Animals were perfused with 1.4% PFA/0.1% glutaraldehyde followed by 4% PFA containing sodium-*m*-periodate and lysine. Brains were removed from the skull and postfixed overnight in the second solution. Fifty-micrometer sections were taken on a vibratome and kept in osmium tetroxide for 1 h. After dehydration, the tissue was immersed in propylene oxide, followed by propylene oxide:Epon (1:1) and finally pure Epon for infiltration. Subsequently, slices were flat-embedded in Epon between two plastic slices. Selected areas from the distal CA3 hippocampal region were cut from the plastic weaver and ultrathin sectioned. After mounting on single-hole copper grids the sections were stained with uranyl acetate and lead citrate and examined under a Zeiss electron microscope.

## ACKNOWLEDGMENTS

We thank K. Jaffuel and J. P. Chauvin for technical help; G. Rougon and Y. Ben-Ari for helpful discussions, encouragement, and support; F. Haigler and X. Morin for critical reading of the manuscript; and M.-C. Tiveron for help with artwork. H.C. was supported by fellowships from EMBO and the European Community TMR program. This work was supported by institutional grants from the CNRS and specific grants from the European Community Biomed program, from the Ligue Nationale Contre le Cancer, and from the Fondation pour la Recherche Medicale.

## REFERENCES

- Acheson, A., Sunshine, J. L., and Rutishauser, U. (1991). NCAM polysialic acid can regulate both cell-cell and cell-substrate interactions. *J. Cell Biol.* **114**: 143-153.
- Amaral, D. G., and Dent, J. A. (1981). Development of the mossy fibers of the dentate gyrus. I. Light and electron microscopic study of the mossy fibers and their expansions. *J. Comp. Neurol.* **195**: 51-86.
- Amaral, D. G., and Witter, M. P. (1995). Hippocampal formation. In *The Rat Nervous System* (G. Paxinos, Ed.), pp. 443-493. Academic Press, San Diego.
- Bally-Cuif, L., Goridis, C., and Santoni, M.-J. (1993). The mouse NCAM gene displays a biphasic expression pattern during neural tube development. *Development* **117**, 543-552.

- Beggs, H. E., Soriano, P., and Maness, P. F. (1994). NCAM-dependent neurite outgrowth is inhibited in neurons from Fyn-minus mice. *J. Cell Biol.* **127**: 825–833.
- Chung, W. W., Lagenaur, C. F., Yan, Y. M., and Lund, J. S. (1991). Developmental expression of neural cell adhesion molecules in the mouse neocortex and olfactory bulb. *J. Comp. Neurol.* **314**, 290–305.
- Cowan, W. M., Stanfield, B. B., and Kishi, K. (1980). The development of the dentate gyrus. *Curr. Top. Dev. Biol.* **15**, 103–157.
- Cremer, H., Lange, R., Christoph, C., Plomann, M., Vopper, G., Roes, J., Brown, R., Baldwin, S., Kraemer, P., Scheff, S., Barthels, D., Rajewsky, K., and Wille, W. (1994). Inactivation of the NCAM gene in mice results in size-reduction of the olfactory bulb and deficits in spatial learning. *Nature* **367**, 455–459.
- Doherty, P., Cohen, J., and Walsh, F. S. (1990a). Neurite outgrowth in response to transfected NCAM changes during development and is modulated by polysialic acid. *Neuron* **5**, 209–219.
- Doherty, P., Fruns, M., Seaton, P., Dickson, G., Barton, C. H., Sears, T. A., and Walsh, F. S. (1990b). A threshold effect of the major isoforms of NCAM on neurite outgrowth. *Nature* **343**, 464–466.
- Edelman, G. M. (1988). Morphoregulatory molecules. *Biochemistry* **27**, 3533–3543.
- Fraser, S. E., Charhart, M. S., Murray, B. A., Choung, C.-M., and Edelman, G. M. (1988). Alterations in the *Xenopus* retinotectal projection by antibodies to *Xenopus* NCAM. *Dev. Biol.* **129**, 217–230.
- Garrity, P. A., and Zipursky, S. A. (1995). Neuronal target recognition. *Cell* **83**, 177–185.
- Goodman, C., and Shatz, C. J. (1993). Developmental mechanisms that generate precise patterns of neuronal connectivity. *Cell/Neuron (Suppl.)* **10**: 77–98.
- Goridis, C., and Brunet, J.-F. (1992). NCAM: Structural diversity, function and regulation of expression. *Semin. Cell Biol.* **3**, 189–197.
- Grenningloh, G., and Goodman, C. S. (1992). Pathway recognition by neuronal growth cones: Genetic analysis of neural cell adhesion molecules in *Drosophila*. *Curr. Opin. Neurobiol.* **2**, 42–47.
- Grenningloh, G., Rehm, J. E., and Goodman, C. S. (1991). Genetic analysis of growth cone guidance in *Drosophila*. Fasciclin II functions as a neuronal recognition molecule. *Cell* **67**, 45–57.
- Haug, F.-M. S. (1973). A light microscopic study in the rat with Timm's sulphide silver method: Methodological considerations and cytological and regional staining patterns. *Adv. Anat. Embryol. Cell Biol.* **47**, 1–71.
- Hu, H., Tomasiewicz, H., Magnuson, T., and Rutishauser, U. (1996). The role of polysialic acid in migration of olfactory bulb interneuron precursors in the subventricular zone. *Neuron* **16**, 735–743.
- Hynes, R. O., and Lander, A. D. (1992). Contact and adhesive specificities in the associations, migrations, and targeting of cells and axons. *Cell* **68**, 303–322.
- Jamot, L., Bertholet, J.-Y., and Crusio, W. E. (1994). Neuroanatomical divergence between two substrains of C57BL/6J inbred mice entails differential radial-maze learning. *Brain Res.* **644**, 352–356.
- Jessell, T. M. (1988). Adhesion molecules and the hierarchy of neural development. *Neuron* **1**, 3–13.
- Kadmon, G., Kowitz, A., Altevogt, P., and Schachner, M. (1990). The neural cell adhesion molecule NCAM enhances L1-dependent cell–cell interactions. *J. Cell Biol.* **110**, 193–208.
- Kaplan, M. S., and Hinds, J. W. (1977). Neurogenesis in the adult rat: Electron microscopic analysis of light radioautographs. *Science* **197**: 1092–1094.
- Key, B., and Akeson, B. (1990). Olfactory neurons express a unique glycosylated form of the neural cell adhesion molecule (NCAM). *J. Cell Biol.* **110**, 1729–1743.
- Kuhn, H. G., Dickinson-Anson, H., and Gage, F. H. (1996). Neurogenesis in the dentate gyrus of the adult rat: Age-related decrease of neuronal progenitor proliferation. *J. Neurosci.* **16**, 2027–2033.
- Landmesser, L., Dahm, L., Schultz, K., and Rutishauser, U. (1988). Distinct roles for adhesion molecules during innervation of embryonic chick muscle. *Dev. Biol.* **130**, 645–670.
- Levitt, P. (1984). A monoclonal antibody to limbic system neurons. *Science* **223**, 299–301.
- Lin, D. M., Fetter, R. D., Kopcynski, N. C., Grenningloh, G., and Goodman, C. S. (1994). Genetic analysis of Fasciclin II in *Drosophila*: Defasciculation, refasciculation and altered fasciculation. *Neuron* **13**, 1055–1069.
- Luthi, A., Laurent, J.-P., Figurov, A., Muller, D., and Schachner, M. (1994). Hippocampal long-term potentiation and neural cell adhesion molecules L1 and NCAM. *Nature* **372**, 777–779.
- Muller, D., Wang, C., Skibo, G., Toni, N., Cremer, H., Calaora, V. C., Rougon, G., and Kiss, J. S. (1996). PSA-NCAM is required for activity induced synaptic plasticity. *Neuron* **17**: 413–422.
- Ono, K., Tomasiewicz, H., Magnuson, T., and Rutishauser, U. (1994). N-CAM mutation inhibits tangential neuronal migration and is phenocopied by enzymatic removal of polysialic acid. *Neuron* **13**, 595–609.
- Pimenta, A. F., Zhukareva, V., Barbe, M. F., Reinoso, B. S., Grimley, C., Henzel, W., Fischer, I., and Levitt, P. (1995). The limbic system-associated protein is an Ig superfamily member that mediates selective neuronal growth and axon targeting. *Neuron* **15**, 287–297.
- Rougon, G. (1993). Structure, metabolism and cell biology of polysialic acids. *Eur. J. Cell Biol.* **61**: 197–207.
- Rousselot, P., Lois, C., and Alvarez-Buylla, A. (1995). Embryonic (PSA) N-CAM reveals chains of migrating neuroblasts between the lateral ventricle and the olfactory bulb of adult mice. *J. Comp. Neurol.* **351**, 51–61.
- Rutishauser, U., and Jessell, T. M. (1988). Cell adhesion molecules in vertebrate neural development. *Physiol. Rev.* **68**, 819–857.
- Rutishauser, U., Acheson, A., Hall, A. K., Mann, D. M., and Sunshine, J. (1988). The neural cell adhesion molecule (NCAM) as a regulator of cell–cell interactions. *Science* **240**, 53–57.
- Schuch, U., Lohse, M. J., and Schachner, M. (1989). Neural cell adhesion molecules influence second messenger systems. *Neuron* **3**, 13–20.
- Schwegler, H., Crusio, W. E., Lipp, H.-P., and Heimrich, B. (1988). Water-maze learning in the mouse covaries with variation in hippocampal morphology. *Behav. Genet.* **18**, 153–165.
- Seki, T., and Arai, Y. (1993a). Highly polysialylated neural cell adhesion molecule (NCAM-H) is expressed by newly generated granule cells in the dentate gyrus of the adult rat. *J. Neurosci.* **13**, 2351–2358.
- Seki, T., and Arai, Y. (1993b). Distribution and possible roles of the highly polysialylated neural cell adhesion molecule (NCAM-H) in the developing and adult central nervous system. *Neurosci. Res.* **17**, 265–290.
- Silver, J., and Rutishauser, U. (1984). Guidance of optic axons in vivo by a performed adhesive pathway on neuroepithelial endfeet. *Dev. Biol.* **106**, 485–499.
- Spacek, J. (1989). Dynamics of the Golgi method: A time-lapse study of the early phases of impregnation in single sections. *J. Neurocytol.* **18**, 27–38.
- Stanfield, B. B., and Trice, J. E. (1988). Evidence that granule cells generated in the dentate gyrus of adult rats extend axonal projections. *Exp. Brain Res.* **72**, 399–406.
- Tang, J., Rutishauser, U., and Landmesser, L. (1994). Polysialic acid regulates growth cone behavior during sorting of motor axons in the plexus region. *Neuron* **13**: 405–414.

- Tessier-Lavigne, M. (1994). Axon guidance by diffusible repellants and attractants. *Curr. Opin. Genet. Dev.* **4**, 596–601.
- Thiery, J. P., Brackenbury, R., Rutishauser, U., and Edelman, G. M. (1977). Adhesion among neural cells of the chicken embryo. II. Purification and characterisation of a cell adhesion molecule from chicken retina. *J. Biol. Chem.* **252**, 6841–6845.
- Tomasiewicz, H., Ono, K., Yee, D., Thompson, C., Goridis, C., Rutishauser, U., and Magnuson, T. (1993). Genetic deletion of a neural cell adhesion molecule variant (N-CAM-180) produces distinct defects in the central nervous system. *Neuron* **11**, 1163–1174.
- Tosney, K. W., Watanabe, M., Landmesser, L., and Rutishauser, U. (1986). The distribution of NCAM in the chick hindlimb during axon outgrowth and synaptogenesis. *Dev. Biol.* **114**, 437–452.
- van Daal, J. H. H. M., Herbergs, P. L., Crusio, W. E., Schwegler, H., Jenks, B. G., Lemmens, W. A. J. G., and van Aberleen, J. H. F. (1991). A genetic-correlation study of hippocampal structural variation and exploration activities in mice. *Behav. Brain Res.* **43**, 57–64.
- Williams, E. J., Furness, J., Walsh, F. S., and Doherty, P. (1994). Activation of the FGF receptor underlies neurite outgrowth stimulated by L1, NCAM, and N-cadherin. *Neuron* **13**, 583–594.
- Yin, X., Watanabe, M., and Rutishauser, U. (1995). Effect of polysialic acid on the behavior of retinal ganglion cell axons during growth into the optic tract and tectum. *Development* **121**, 3439–3446.
- Zhang, H., Miller, R. H., and Rutishauser, U. (1992). Polysialic acid is required for optimal growth of axons on a neuronal substrate. *J. Neurosci.* **12**, 3107–3114.

Received October 29, 1996

Revised November 8, 1996

Accepted November 8, 1996